International Journal of Civil Engineering

Structure
Earthquake

An investigation on seismic design indicators of RC columns using finite element analyses

G. Arslan[1,*], M. Hacisalihoglu[2], M. Balci[2], M. Borekci[2]

Received: September 2012, Revised: October 2013, Accepted: November 2013

Abstract

The main cause of structural damage in buildings subjected to seismic actions is lateral drift. In almost all reinforced concrete (RC) structures, whether designed with walls or frames, it is likely to be the code drift limits that control the design drift. The design drift limits and their contribution to damage may be represented indirectly through the material strain limits. The aim of this study is to investigate the seismic design indicators of RC columns using finite element analyses (FEA). The results of FEA have been compared with the results of experimental studies selected from literature. It is observed that the lateral load-deflection curves of analyzed columns are in agreement with the experimental results. Based on these lateral load-deflection curves, the drift limits and the material strain limits, given by the codes as performance indicator, are compared. It is observed that the material strain limits are non-conservative as performance indicator of RC columns, compared to the drift limits.

Keywords: *Reinforced concrete, Column, Seismic design, Drift limits, Material strain limit, Structural damage.*

1. Introduction

Performance-based seismic design has been the subject of significant research activity among the earthquake engineering community for over two decades [1]. In general, performance-based seismic design relies on the identification of structural performance expressed in terms of limit states that are often defined on the basis of material strain, drift or displacement. Curvature capacity at the cross-sectional level and drift capacity at the member level are often used as criteria for evaluating the performance of the column. Priestley and Kowalsky [2] and Kowalsky [3] have defined expressions for curvatures and drifts based on material strains. Brachmann et al. [4] proposed a direct relationship between the limiting drift ratio and the corresponding material and structural properties of RC columns and Kabeyasawa [5] and Mostafaei et al. [6] presented approaches for displacement–based analysis of RC columns and estimation of ultimate deformation and load capacity of RC columns based on principles of axial-shear-flexure interaction. Barrera et al. [7] investigated the deformation capacity of slender RC columns under monotonic flexure and constant axial load based on Barrera et al.'s [8] experimental study.

According to the Turkish Earthquake Code (TEC) [9] and FEMA356 [10], based on relative storey drift ratio, three limit conditions are defined for ductile elements. Also, the TEC [9] defines the upper bounds (capacity) of deformation for different sectional damage thresholds for the ductile load-bearing system components that undergo plastic deformations. The relationship between storey drift ratio and material strains is important because damage is often assumed to be well correlated with concrete compression and steel tension strain levels.

The capacity and behavior of the columns of a RC frame structure are important factors that determine the seismic performance of the whole structure [11]. Seismic performance assessment has become more important than ever since structural designers started to employ performance based design methods, which require predicting structural and member behaviors at different limit states precisely. The damage level of the columns subjected to an earthquake is essential for predicting the seismic vulnerability of a RC frame structure. Jiang et al. [12] proposed a semi-empirical method to estimate lateral displacements of flexure-dominant rectangular RC columns at a number of key seismic damage states. Erduran and Yakut [13] have developed displacement-based damage functions for the components of RC

* *Corresponding author: gurayarslan@yahoo.com, aguray@yildiz.edu.tr*

1 Associate Proffesor, PhD, Yıldız Technical University, Faculty of Civil Engineering, Civil Engineering Department, Structural Engineering Division, 34210 Davutpasa-Esenler-Istanbul, Turkey

2 Ms, Yıldız Technical University, Civil Engineering Department, Structural Engineering Division, 34210 Davutpasa-Esenler-Istanbul, Turkey

moment resisting frames using finite element analyses. The seismic demands are obtained by a nonlinear analysis or a pushover analysis [10, 14] of the structure subjected to monotonically increasing lateral forces until a target value of roof deflection is reached.

It is generally accepted that damage is strain related (for structural components), or drift related (for non-structural components). The damage-control limit state can also be defined by material strain limits and by design drift limits intended to restrict non-structural damage. The material strain limits would be compared with the code drift limits imposed to limit non-structural damage, and the more critical adopted for design. The aim of this study is to investigate strain values for RC columns based on the drift ratio, defined as the ratio of the difference between the deflections of the two ends of the column to the column height. To develop consistent and reliable damage-drift relations, a number of finite element analyses (FEA) were carried out for RC columns using the software ANSYS [15]. In order to validate the finite element model, a column tested previously by Lin and Lin [16], Atalay and Penzien [17] and Lu et al. [18] was modeled first. Upon verifying that the finite element model represents the actual behavior adequately, strain values corresponding to the drift ratios defining damage levels -minimum damage limit, safety limit and collapsing limit- were compared with the strain limits given by the TEC [9] for each damage level.

2. Specimen Details of RC Columns

The first step of the numerical investigations was the verification of the finite element model. For this purpose, Lin and Lin [16], Atalay and Penzien [17] and Lu et al.'s [18] columns were modeled and analyzed (Fig. 1). The shear strengths of the columns were much greater than their flexural strengths so that the columns were enforced to fail in pure flexure.

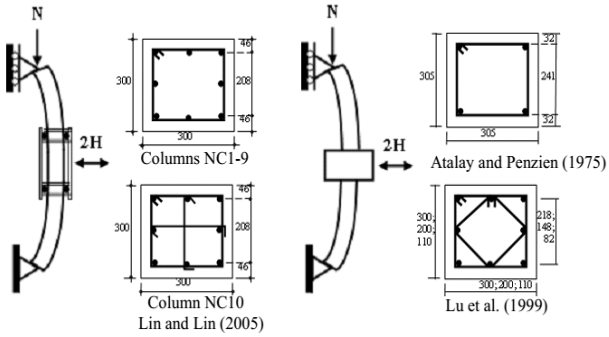

Fig. 1 Test setups (double ended) and details of columns (unit: mm)

Specimen details required for the modeling of the RC columns are given in Table 1, where f_c is the compressive strength of concrete, N/N_o is the ratio of the applied axial load (N) to the axial load capacity (N_0), a/d is the span-to-depth ratio, s is the spacing of transverse reinforcement, s_c is the spacing of transverse reinforcement in confinement zones, f_{yv} is the yield strength of transverse reinforcement, f_y is the yield strength of longitudinal reinforcement, $\rho_s f_{yv}$ is the nominal transverse reinforcement strength, and ρ is the longitudinal reinforcement ratio.

Table 1 Specimen details of RC columns

Column name	f_c (MPa)	N/N_o	a/d	s [s_c] (mm)	f_{yv} (MPa)	$\rho_s f_{yv}$ (MPa)	ρ	f_y (MPa)	Section size (mmxmm)
NC1[a]	50.0	0.20	4.09	100	452.1	5.11	0.0338	438	300x300
NC2[a]	50.5	0.40	4.09	100	452.1	5.11	0.0338	438	300x300
NC3[a]	50.2	0. 60	4.09	100	452.1	5.11	0.0338	438	300x300
NC4[a]	31.8	0.20	4.09	100	452.1	5.11	0.0338	438	300x300
NC5[a]	57.6	0.20	4.09	100	452.1	5.11	0.0338	438	300x300
NC6[a]	49.0	0.20	4.09	130	452.1	3.93	0.0338	438	300x300
NC7[a]	50.6	0.20	4.09	70	452.1	7.05	0.0338	438	300x300
NC8[a]	48.5	0.20	4.09	100	365.2	4.24	0.0338	438	300x300
NC9[a]	49.1	0.20	4.09	100	554.6	5.71	0.0338	438	300x300
NC10[a]	49.7	0.20	4.09	100	452.1	5.88	0.0338	438	300x300
1S1[b]	29.1	0.10	5.50	76	363	5.59	0.0167	367	305 x 305
2S1[b]	30.7	0.09	5.50	127	363	3.38	0.0167	367	305 x 305
3S1[b]	29.2	0.10	5.50	76	363	5.59	0.0167	367	305 x 305
4S1[b]	27.6	0.10	5.50	127	363	3.38	0.0167	429	305 x 305
6S1[b]	31.8	0.18	5.50	127	392	3.65	0.0167	429	305 x 305
10[b]	32.4	0.27	5.50	127	392	3.65	0.0167	363	305 x 305
12[b]	31.8	0.27	5.50	127	373	3.47	0.0167	363	305 x 305
C2L1[c]	33.4	0.07	5.44	27 [60]	181	2.31	0.0179	462	300 x 300
C3L2[c]	29.3	0.20	5.35	60	181	0.97	0.0226	462	200 x 200
C5L2[c]	27.4	0.20	5.23	40	195	0.55	0.0187	475	110 x 110

$N_o = 0.85 f_c (A_g - A_{st}) + A_{st} f_{yh}$

[a]Lin and Lin [16]; [b]Atalay and Penzien [17]; [c]Lu et al. [18]

3. Finite Element Modeling of RC Columns

In the numerical investigations carried out within the scope of this study, the finite element software ANSYS [15] was used. A perfect bond is assumed between the reinforcement and the concrete components implying compatible deformation. A load-controlled analysis was performed by increasing the load at the tip of the column incrementally. The deflection was then calculated at each step. Only the half of the column was modeled due to the symmetry of the loading and geometry. The analysis was carried out using Newton-Raphson technique.

Reinforcements based on the effects of strain hardening effect were modeled discretely using Link8 element. Solid45 elements have been used at the supports and at the loading regions to prevent stress concentrations at those regions. The concrete has been modeled using Solid65 eight-node brick element, which is capable of simulating the cracking and crushing behavior of brittle materials. The Solid65 element requires linear isotropic and multiaxial isotropic material properties to properly model the concrete.

The tensile strength f_t of concrete is assumed as $f_t = 0.3 f_c^{2/3}$ [19, 20], the modulus of elasticity E_c is taken as $4730\sqrt{f_c}$ [21] for normal-strength concrete and $E_c = 3320\sqrt{f_c} + 6900$ [22] for high-strength concrete.

The nonlinear analyses of the columns were performed by employing the Drucker–Prager yield criterion for concrete. The crack interface shear transfer coefficient for open cracks is assumed to take a value of 0.5 while it is assumed to take a value of 0.9 for closed cracks. The Drucker–Prager criterion is a generalization of the Mises criterion. The failure occurs when the Drucker–Prager cone crosses the surface. By failure, it is meant either the actual failure caused by unstable crack growth or the onset of softening material response, with the localization of deformation into a shear band.

3.1. Principle and modeling parameters of the drucker–prager criteria

The Drucker–Prager yield criterion can be used to describe the ductile behavior of the materials, which are weak in tension and exhibit volumetric plastic strain. The Drucker–Prager yield criterion can be written as [23].

$$f(I_1, J_2) = \alpha I_1 + \sqrt{J_2} - k = 0 \tag{1}$$

in which I_1 is the first stress invariant, J_2 is the second stress invariant, α and k are material constants which can be related to the friction angle ϕ and cohesion c of the Mohr–Coulomb criterion in several ways. We shall assume that the Drucker–Prager cone circumscribes the Mohr–Coulomb hexagonal pyramid, and the material constants α and k are obtained as [23]:

$$\alpha = \frac{2\sin\phi}{\sqrt{3}(3-\sin\phi)} \quad k = \frac{6c\cos\phi}{\sqrt{3}(3-\sin\phi)} \tag{2}$$

The internal friction angle is approximately between 30˚ and 37˚, which can be found by drawing various tangent lines to the compressive meridian, obtained from the experimental data. These values have been successfully used in the previous studies [23-25]. In this study, internal friction angles for normal and high-strength concrete are considered as 33˚ and 37˚, respectively.

4. Comparison of the Results of FEA with the TEC Requirements

4.1. Evaluation of the results of FEA

In the past, much experimental research has been conducted on the inelastic behaviour of RC columns [16-18]. However, only a few of them presented the material strain values during experimental tests [16]. Load-deflection curves and material strain values taken from nonlinear FEA have been verified using Lin and Lin's [16] column test results.

The lateral load (H) versus deflection (δ) curves obtained through FEA are plotted in Fig. 2. The numerical and experimental results match fairly well. The numerical load–deflection curve was obtained from a pushover analysis, which is a one-way static procedure. However, the test was carried out under hysteretic loading. It is observed in Fig. 2 that the load carrying capacities of NC7, and 1S1 columns are different in the positive and negative directions. The results of FEA are in agreement with the envelope curve in the direction where the maximum load carrying capacity is reached.

The relative drift ratio corresponding to each damage level was determined using the load–deflection curves of columns tested under cyclic loading rather than the capacity curves of the columns. To determine the relative drift ratios of the RC columns, the test data of 20 RC columns [16-18] were used.

According to the TEC [9] and FEMA356 [10], the damage boundary mainly depends on lateral drift levels. Basically, three limit conditions have been defined for ductile elements in terms of the drift corresponding to the load carrying capacity of the column. The damage boundaries based on the TEC [9] and FEMA356 [10] will be discussed in detail in Section 4.2.

The relative drift ratios defining damage boundaries based on linear elastic analyses are defined in the TEC [9]. The section strain capacities corresponding to the relative drift ratios obtained from FEA can be compared with the section strain capacities defined in the TEC [9] since the deflections obtained from FEA agree with those obtained via experiments.

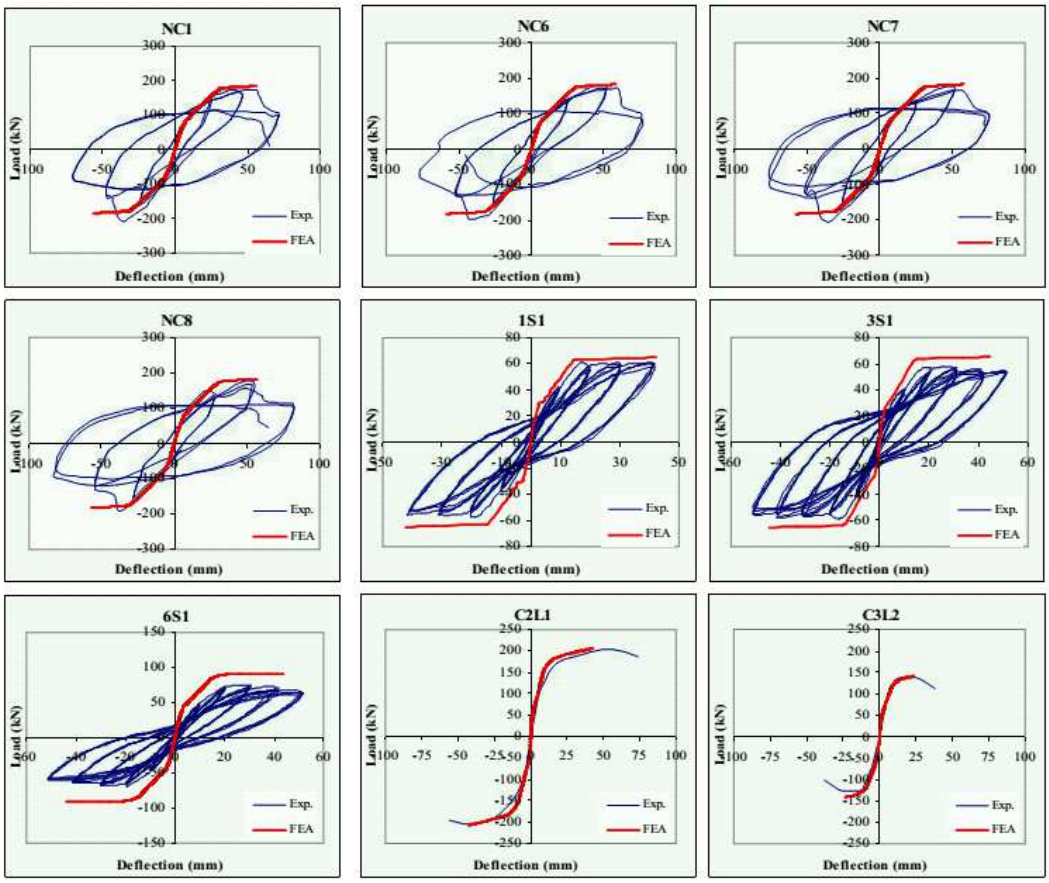

Fig. 2 Load–deflection curves for columns

4.2. Definition of damages in cross sections and elements

The principal damage states include yielding, crushing of concrete cover, significant concrete spalling, buckling of longitudinal bar, and ultimate limit state. According to Matamoros and Sozen [26], and Lehman et al. [27], spalling of the concrete cover occurs after a yielding of the longitudinal reinforcement under cyclic loading. Subsequently, buckling or fracture of longitudinal bars may occur, which causes failure of the column. According to the TEC [9] and FEMA356 [10], three limit conditions are defined for ductile elements. These are *Minimum Damage Limit* (MN), *Safety Limit* (GV) and *Collapsing Limit* (GC)**.** MN defines the beginning of the behavior beyond elasticity, GV defines the limit of the behavior beyond elasticity that the section is capable of safely ensuring the strength, and GC defines the limit of the behavior before collapsing. Elements that the damages with critical sections do not reach MN are within the *Minimum Damage Region*, those in-between MN and GV are within *Marked Damage Region*, those in-between GV and GC are in *Advanced Damage Region*, and those going beyond GC are within *Collapsing Region.*

In the analyses performed using linear-elastic methods in each earthquake direction, relative storey drifts of columns, beams or walls in each storey of the building shall not exceed the value given in Table 2.

Table 2 Boundaries of relative storey drift

Damage boundary	Relative drift ratio (δ / h)	
	TEC [9]	FEMA356 [10]
MN	0.01	0.01
GV	0.03	0.02
GC	0.04	0.04

According to the TEC [9], the upper bounds (capacity) of deformation for different sectional damage thresholds for the ductile load-bearing system components that undergo plastic deformations are defined below:

For *Minimum Sectional Damage Boundary (MN)*, upper bounds of the concrete strain in the outmost fiber of the section and the reinforcement steel strain volitions:

$$(\varepsilon_{cu})_{MN} = 0.0035\,;(\varepsilon_s)_{MN} = 0.010 \tag{3}$$

in which ε_{cu} and ε_s are strain of concrete pressure in the outermost fibrous of the section of the cross section and strain of reinforcement steel, respectively.

For Section *Security Bound (GV)*, upper bounds of the concrete pressure strain in the outmost fiber of hoop and the reinforcement steel strain volitions:

$$\begin{aligned} &\left(\varepsilon_{cg}\right)_{GV} = 0.0035 + 0.01(\rho_s / \rho_{sm}) \le 0.0135\,; \\ &(\varepsilon_s)_{GV} = 0.040 \end{aligned} \tag{4}$$

in which ε_{cg} is strain of concrete pressure in the outermost fibrous of the section inside of the lateral reinforcement binders.

For Section *Collapse Bound* (GC), upper bounds of the concrete strain in the outmost fiber of hoop and the reinforcement steel strain volitions:

$$\begin{aligned} &(\varepsilon_{cg})_{GC} = 0.004 + 0.014(\rho_s / \rho_{sm}) \le 0.018; \\ &(\varepsilon_s)_{GC} = 0.060 \end{aligned} \quad (5)$$

4.3. Evaluation of the FEA results with performance limits of the TEC

According to the TEC [9], the general principle of earthquake-resistant design is to prevent structural and non-structural elements of buildings from any damage under low intensity earthquakes; to limit the damage in structural and non-structural elements to repairable levels under medium-intensity earthquakes, and to prevent the overall or partial collapse of buildings under high-intensity earthquakes in order to avoid the loss of life. Determining the structural performances of the buildings under seismic effect and for the strengthening purposes, effect / capacity ratio of beam, column and wall sections are defined according to the damage limits.

4.3.1. Minimum damage limit (MN)

The deflections of columns obtained via FEA are the ones at the point of lateral loading. The ratio of the deflection at the point of loading to the distance between the point of loading and support is defined as relative drift ratio (δ / h). The compressive strain in the outermost concrete fiber of the cross section (ε_{cu}) corresponding to the relative drift ratio of 0.01 was found to be lower than 0.0035 for NC1, NC3-5, NC7-10, 2S1, 3S1, while it is higher than 0.0035 for the other columns.

According to Eurocode 8 [28] and ASCE/SEI 41 [29], minimum damage level is defined as the yielding of tensile reinforcement. Based on this definition, ε_{cg} was found to be 0.0010~0.0242 in the analyses, where the average value of ε_{cg} for 20 columns is 0.0021 (Fig. 3).

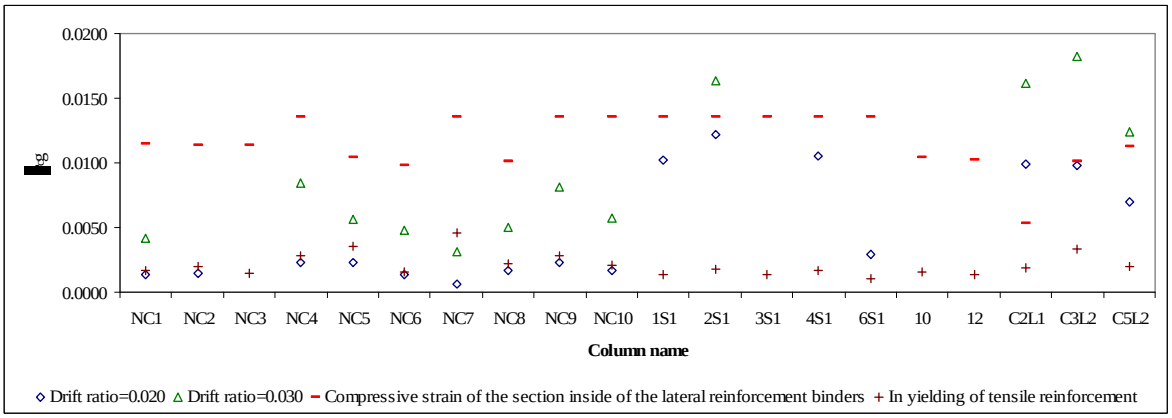

Fig. 3 Comparison of FEA results and GV boundary by the TEC

4.3.2. Safety limit (GV)

The compressive strain in the outermost concrete fiber of the section inside of the lateral reinforcement binders (ε_{cg}) and the tensile strain in the reinforcement (ε_s) were obtained from analyses corresponding to the relative drift ratio of 0.03 for GV. The damage boundary GV defined by the TEC [9] are compared in Fig. 3. Eq. (4) defines the upper bounds for ε_{cg} and ε_s according to the TEC [9].

ε_{cg} corresponding to the relative drift ratio of 0.03 was found to be 0.0032~0.0182 for NC1, NC4-10, 2S1, C2L1, C3L2, C5L2, while the other columns collapsed at relative drift ratios less than 0.03. The values of ε_{cg} are generally below the boundary given by Eq. (4) (Fig. 3). Based on these results for $(\delta / h) = 0.03$, it can be suggested to decrease the upper bound for ε_{cg} defined by the TEC.

ε_{cg} corresponding to the relative drift ratio of 0.02 was found to be 0.0007~0.0286 for NC1, NC2, NC4-10, 1S1, 2S1, 4S1, 6S1, C2L1, C3L2, C5L2, while the other columns collapsed at relative drift ratios less than 0.02. The values of ε_{cg} are below the boundary given by the TEC (Fig. 3). Based on these results for $(\delta / h) = 0.02$, it can be suggested to decrease the upper bound for ε_{cg}.

4.3.3. Collapsing Limit (GC)

Fig. 4 shows the results of FEA with the limiting value of ε_{cg} for collapse state, defined by the TEC. ε_{cg} was found to be 0.0015~0.0196, where the average value of ε_{cg} is 0.0099, which is below the maximum boundary given by the TEC as 0.018. Based on these results, it can be suggested to decrease the upper bound for ε_{cg} defined by the TEC.

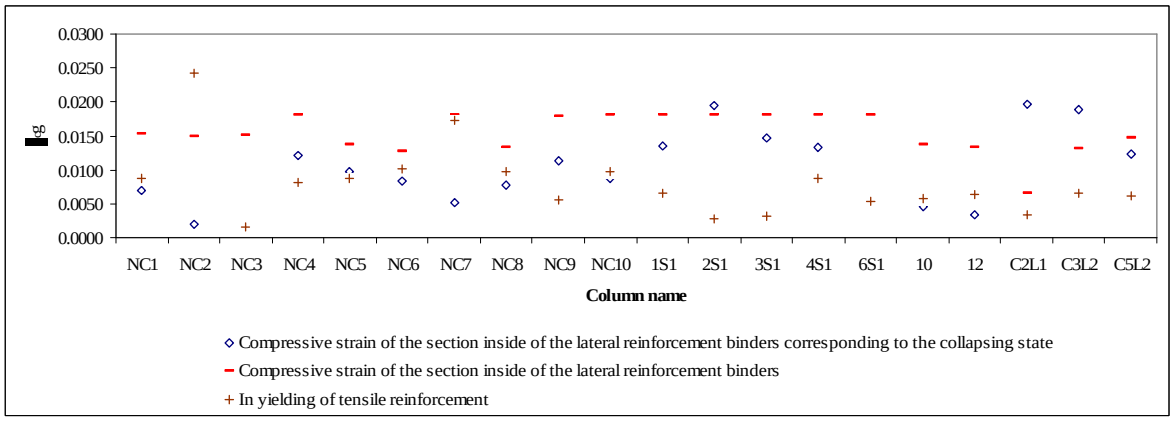

Fig. 4 Comparison of FEA results and GC boundary by the TEC

ε_s corresponding to the collapse state for 20 columns was found to be ~0.0088 in the analyses, which is far below the boundary given by the TEC as 0.06. In the experimental studies conducted by Lin and Lin [16], ε_s was found to be 0.0021~0.0073, where the average value of ε_s is 0.0044. The values of ε_s obtained from FEA were found to be 0.0021~0.0082. The average value of ε_s for Lin and Lin's [16] columns is 0.0051. It is observed that the values of ε_s obtained from FEA are in agreement with the experimental results. It should be noted that the global collapse of a structure is not only related to collapse of an individual column.

According to ICC [30] and ICBO [31], a storey drift capacity of 2.0 to 2.5% is expected for special moment-resisting RC frames designed for seismic effects. In this regard, a lateral drift ratio of 2.5% is used as the target value for deformation. Fig. 5 shows that none of the performance-based design expressions considered in this study guarantees a drift capacity of 2.5%.

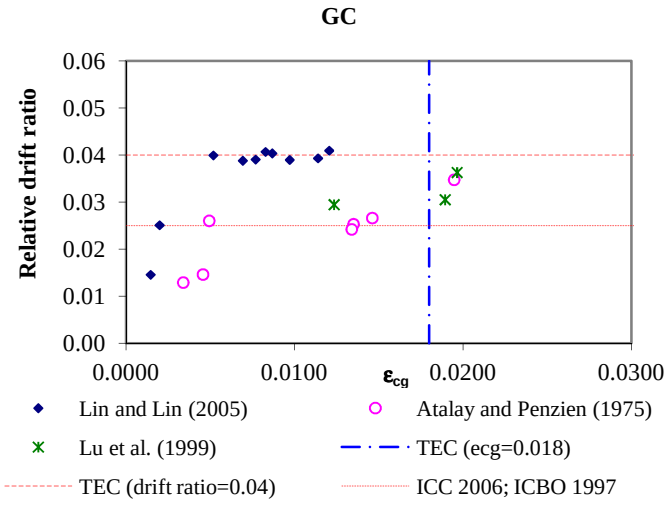

Fig. 5 ε_{cg} - Relative drift ratio corresponding to the collapse state

5. Conclusions

Considering that the results of nonlinear FEA on RC columns are in agreement with the experimental results, the performance of RC columns subjected to lateral loading is summarized below.

Minimum Damage Limit;

For the relative drift ratio equal to 0.01, the compressive strain in the outermost concrete fiber of the cross section, ε_{cu}, is far above the boundary given by the TEC [9] as 0.0035.

Minimum damage level is defined as the yielding of tensile reinforcement by Eurocode 8, and ASCE/SEI 41. Based on this definition, the average value of ε_{cg} for 20 columns was found to be 0.0021.

Safety Limit;

For the relative drift ratio equal to 0.02 and 0.03, the compressive strain in the outermost concrete fiber of the section inside of the lateral reinforcement binders, ε_{cg}, and the tensile strain in the reinforcement, ε_s, were found to be below the boundary given by the TEC. Based on these results, it can be suggested to decrease the upper bound for ε_{cg}.

The upper bound for the tensile strain in the

reinforcement is given as $\varepsilon_s = 0.04$ by the TEC. ε_s obtained from FEA is around 0.0070, which is far below the boundary given by the TEC and shows that the reinforcement yields.

Collapsing Limit;

ε_{cg} was found to be 0.0015~0.0196, where the average value of ε_{cg} is 0.0099, which is below the boundary given by the TEC (Eq. (4)).

ε_s corresponding to the collapsing state was found to be ~0.0088 in the analyses, which is far below the boundary given by the TEC as 0.06. For the ratio of relative storey drift equal to 0.04, ε_{cg} and ε_s were found to be far below the boundaries given by the TEC. However, the behaviour of the whole structure is not necessarily the same as the behaviour of an individual column. This study focuses on the behaviour of columns individually, so it neglects the effect of other frame elements.

According to ICC [30] and ICBO [31], a storey drift capacity of 2.0 to 2.5% is expected for special moment-resisting RC frames designed for seismic effects. The results show that none of the performance-based design expressions considered in this study guarantees a drift capacity of 2.5%.

Since the number of columns analyzed in this study is limited, it is proposed that the boundaries given by the TEC may be revised after more columns are analyzed.

References

[1] Vidot-Vega AL, Kowalsky MJ. Relationship between strain, curvature, and drift in reinforced concrete moment frames in support of performance-based seismic design, ACI Structural Journal, 2010, N0. 3, Vol 107, pp. 291-299.

[2] Priestley MJN, Kowalsky MJ. Aspects of drift and ductility capacity of cantilever structural walls, Bulletin of the New Zealand National Society for Earthquake Engineering, 1998, No. 2, Vol. 31, pp. 73-85.

[3] Kowalsky M. Deformation limit states for circular reinforced concrete bridge columns, Journal of Structural Engineering, 2000, No. 8, Vol. 126, pp. 869-878.

[4] Brachmann I, Browning J, Matamoros A. Drift-dependent confinement requirements for reinforced concrete columns under cyclic loading, ACI Structural Journal, 2004, No. 5, Vol. 101, pp. 669-677.

[5] Mostafaei H, Kabeyasawa T. Axial-shear-flexure interaction approach for reinforced concrete columns, ACI Structural Journal, 2007, No. 2, Vol. 104, pp. 218-226.

[6] Mostafaei H, Vecchio FJ, Kabeyasawa T. Deformation capacity of reinforced concrete columns, ACI Structural Journal, 2009, No. 2, Vol. 106, pp. 187-195.

[7] Barrera AC, Bonet JL, Romero ML, Fernández MA. Ductility of slender reinforced concrete columns under monotonic flexure and constant axial load, Engineering Structures, 2012, No. 12, Vol. 40, pp. 398–412.

[8] Barrera AC, Bonet JL, Romero ML, Miguel PF. Experimental tests of slender reinforced concrete columns under combined axial load and lateral force, Engineering Structures, 2011, No. 12, Vol. 33, pp. 3676–89.

[9] Turkish Earthquake Code. Specification for structures to be built in disaster areas, Ministry of Public Works and Settlement Government of Republic of Turkey, Ankara, 2007.

[10] FEMA356: 2000, Prestandart and Commentary for The Seismic Rehabilitation of Buildings, Federal Emergency Management Agency, Washington DC.

[11] Balci M, Arslan G. An investigation on minimum damage limit of RC columns using finite element analyses, 14th ECEE, Ohrid, Republic of Macedonia, 2010.

[12] Jiang H, Lu X, Kubo T. Damage displacement estimation of flexure-dominant RC columns, Advances in Structural Engineering, 2010, No. 2, Vol. 13, pp. 357-368.

[13] Erduran E, Yakut A. Component damage functions for reinforced concrete frame structures, Engineering Structures, 2007, Vol. 29, pp. 2242–2253.

[14] ATC40: 1996, Seismic evaluation and retrofit of concrete buildings, Report No. SSC 96-01, California Seismic Safety Commission, Applied Technology Council, California.

[15] ANSYS 11.0: 2007, Theory Reference Manual.

[16] Lin C.H, Lin SP. Flexural behavior of high-workability concrete columns under cyclic loading, ACI Structural Journal, 2005, No. 3, Vol. 102, 412-421.

[17] Atalay MB, Penzien J. The seismic behavior of critical regions of reinforced concrete components as influenced by moment, shear and axial force, Report No. EERC 75-19, University of California, Berkeley, 1975, 226 p.

[18] Lu Y, Vintzileou E, Zhang GF, Tassios TP. Reinforced concrete scaled columns under cyclic actions, Soil Dynamics and Earthquake Engineering, 1999, Vol. 18, pp. 151-167.

[19] European Committee for Standardization (CEN), Design of concrete structures, Part 1: General rules and rules for buildings, Eurocode 2, Brussels, 1992.

[20] Concrete Society Technical (CST) Report 49: Design guidance for high strength concrete, UK, 1998, 168 p.

[21] ACI Committee 318: Building code requirements for structural concrete (ACI 318M–08) and commentary, ACI, Farmington Hills, MI, 2008, 473 p.

[22] ACI Committee 363R-92: State-of-the-art report on high-strength concrete, Reported by ACI Committee 363, Farmington Hills, MI, 1997.

[23] Chen WF. Plasticity in Reinforced Concrete, McGraw-Hill Company, 1982.

[24] Arslan G. Sensitivity study of the Drucker–Prager modeling parameters in the prediction of the nonlinear response of reinforced concrete structures, Material and Design, 2007, No. 10, Vol. 28, pp. 2596–603.

[25] Arslan G, Hacısalihoglu M. Nonlinear analysis of RC columns using the Drucker–Prager model, Journal of Civil Engineering and Management, 2013, No. 1, Vol. 19, pp. 69-77.

[26] Matamoros AB, Sozen MA. Drift limits of high-strength concrete columns subjected to load reversals, Journal of Structural Engineering, 2003, No. 3, Vol. 129, pp. 297–313.

[27] Lehman D, Moehle J, Mahin S, Calderone A, Henry L. Experimental evaluation of the seismic performance of reinforced concrete bridge columns, Journal of Structural Engineering, 2004, No. 6, Vol. 130, pp. 869–879.

[28] Eurocode 8: 2005, Design of Structures for Earthquake Resistance—Part 3: Assessment and Retrofitting of Buildings, Comité Européen de Normalisation, Brussels, Belgium, 89 p.

[29] ASCE/SEI 41, Seismic Rehabilitation of Existing Buildings, ASCE, Reston, VA, 2007, 416 p.

[30] International Code Council (ICC): International Building Code, Falls Church, VA, 2006, 663 p.

[31] International Conference of Building Officials (ICBO): Uniform Building Code, Structural Engineering Design Provisions, Whittier, CA, 1997, Vol. 21, 492 p.